Assessment of ductility properties of the connections in a prefabricated timber panel

D. P. Pasca
Faculty of Science and Technology, Norwegian University of Life Sciences, Ås, Norway
C. A. Myrvhold
Faculty of Science and Technology, Norwegian University of Life Sciences, Ås, Norway
O. A. Høibø
Faculty of Environmental Science and Natural Resource Management, Norwegian University of Life Sciences, Ås, Norway
A. Q. Nyrud
Faculty of Environmental Science and Natural Resource Management, Norwegian University of Life Sciences, Ås, Norway
R. Tomasi
Faculty of Science and Technology, Norwegian University of Life Sciences, Ås, Norway

This study presents the results of an experimental testing regime conducted on the joints of a wood-based prefabricated sandwich panel recently developed in Norway. The connections investigated were those involved in constituting the lateral force-resisting system for a wall assembly, namely the panel-to-sill connection. Several European standards are undergoing a revision process, amongst them the one that describes the procedures and methods of assessment of timber joints made with mechanical fasteners, tested under quasi-static cyclic conditions. The objective of this investigation was therefore to compare the current methodologies with those presented in a revision proposal and a third method used in Japan. The revision proposal introduces the concept of strength degradation, which should ensure a large amount of energy dissipation without a significant loss of strength, when designing structures for earthquake loads. The results of the testing regime are presented, and advantages and disadvantages of the methods are discussed.

1. Introduction

During the last decade, timber buildings have become an attractive alternative to systems built with other materials as concrete, steel and masonry. Although the main reason of the increasing popularity of timber structural systems is related to the growing interest in sustainable building, timber products also have proven excellent performance in relation to speed of construction and an excellent capacity to withstand earthquakes loads.

The high demand for timber buildings in the recent past, have driven the industry to conceive an increasing number of new engineered timber products. These products are more and more often prefabricated elements which are assembled on-site. In this context, the role played by those standards that specifies the test methods for timber structures, is very important. The behaviour of a timber structure under lateral cyclic loads (e.g. wind and earthquake loads) is mainly governed by the response of its connection systems, (as showed by several studies Piazza *et al.* (2011), Piazza *et al.* (2015)). Furthermore, joints and assemblages made with mechanical fasteners for load-bearing timber elements in seismic regions in Europe, need to be tested according to EN 12512:2001+A1:2005. This is because information about properties such as ductility, dissipation of energy and impairment of strength are needed in order to design according to EN 1998-1:2004/A1:2013. Such parameters are determined from the analysis of the load-displacement curve of a destructive test. However, as already pointed out by other authors (Muñoz *et al.* (2008)), the definition of the ductility is strongly dependent on the evaluation of the yield point and the definition of failure load. The load-displacement curve, in timber assemblies, is characterised by a non-linear trend much more marked compared for example to steel assemblies. Seldom in fact there is an unambiguous transition from the elastic range to the plastic range with two well defined linear parts. An experimental regime on a product recently developed in Norway gave the opportunity to compare how different methods influence the calculation of the yield point and ductility ratio. Some preliminary results of this experimental regime are presented in Pasca *et al.* (2019).

2. Materials and Methods

2.1. Materials and geometry

The tested elements consist of two outer parallel-aligned multilayer solid wood panels, see Fig. 1. Wooden dowels are used to connect the outer layers to each other, these are arranged along two rows in the longitudinal direction of the element with a spacing of 500 mm (S). The elements are produced with a standard width of 200 mm (B), and are manufactured primarily in standard thicknesses ranging from 130 mm to 330 mm (T). The element length is adjusted to the actual floor height up to max 3 m (L). The prefabricated elements are then aligned and connected to a continuous top and bottom sill on site. The panels may be used as exterior and interior bearing walls in residential buildings, or other specific uses, up to three floors Termowood (2007). The elements can also be used to renovate older buildings. Fig. 1 shows the details of an assembled wall.

Several tests were conducted upon different configurations so as to identify which one yields the best performance. The forces of interest were the horizontal (shear) forces acting on the assemblies at the interface between the panels and the (top and bottom) sills, see red lines and arrows in Fig. 1. Type of fastener (screws and nails), their inclination (90°and 60°, with respect to the vertical axes) and type of sill (Solid Wood Panel and solid timber) were the different variables tested. It need to be clarified that the inclination of the fasteners was actually not relevant for this specific test set-up, as the connectors remained in any case perpendicular to the shear plane, and therefore the withdrawal capacity of the screw was not activated. The inclination was however needed to perform another kind of investigation where uplift forces were applied to the specimens.

The Termowood (TW) element is made of two Solid Wood Panels (SWP) according to EN 13353:2008+A1:2011. The SWP in the elements is a 40 mm thick, three-layered wood panel, and the two SWP panels are connected through wood dowels in the middle. The tested top- and bottom-middle sill where made either with solid timber (ST) strength grade C24, according to EN 338:2016, or SWP according to EN 13353:2008+A1:2011.

Two kind of connectors were used to assemble the specimens, both provided by Motek. Screws with external coating C4, partially threaded, type 17 point, with size 5,0x90mm; and diamond coated barbed shank, nails with size 3,1x90mm. Both types of connectors were tested with two different orientations, i.e. 90°and 60°, with respect to the orientation of the external panels.

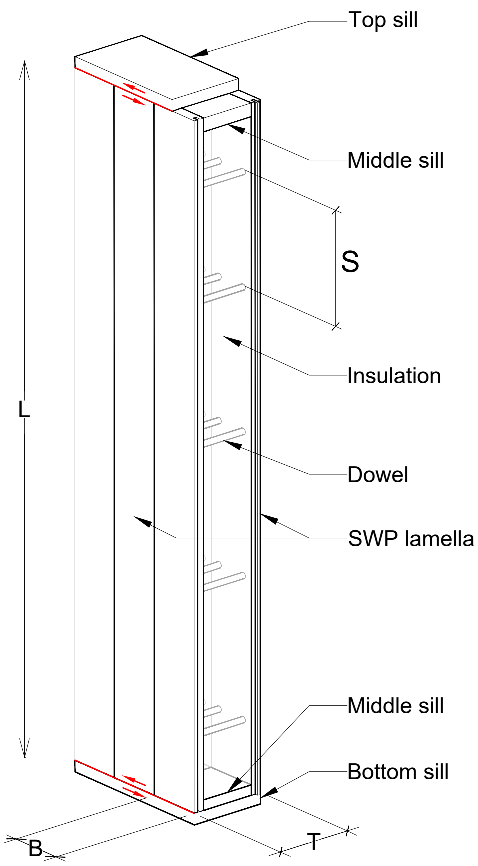

Figure 1. Construction details of Termowood wall. Source:Termowood (2017)

The geometry of the test specimens is shown in Fig. 2 (the dimensions are expressed in mm). The test specimens were set up with two sills with the Termowood element in-between. Two connectors were placed on each side of the element, resulting in eight connectors for each test specimen.

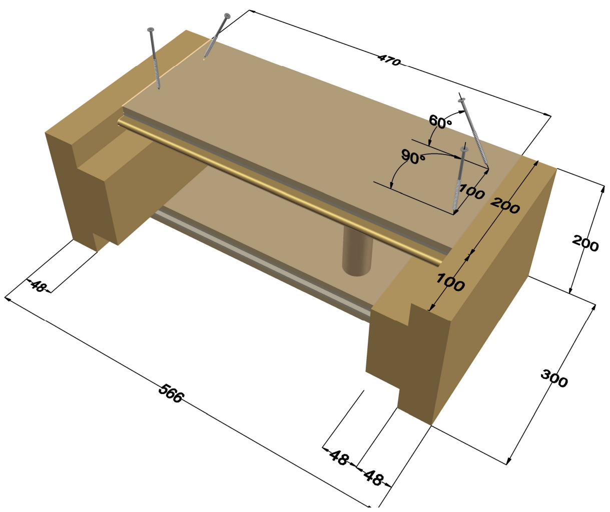

Figure 2. Specimen layout

Each specimen was assembled by the producer, who followed their own internal quality check, and further stored for at least four weeks in a laboratory with controlled climate at 20°C and 65% humidity before testing. The conditioning was according to ISO 554:1976.

2.2. Evaluation of the mechanical properties for cyclic tests

The mechanical properties evaluated from cyclic tests are calculated from the load envelope curve of the hysteresis curve. The main ones are:

- Maximum force
- Yield point
- Ultimate displacement
- Ductility ratio

In order to post-process the data from the cyclic tests three different methods were used:

1. The procedure provided by the EN 12512:2001+A1:2005 standard (from now on referred as 1/6 procedure).
2. The Yasumura & Kaway method (Yasumura (1997)) (from now on referred as Y & K procedure).
3. A modified EEEP method (Casagrande *et al.* (2019)) (from now on referred as EEEP procedure).

2.2.1. EN 12512

EN 12512:2001+A1:2005 is the current standard to perform cyclic tests on timber joints made with mechanical fasteners. It provides the protocol to perform such tests and furthermore two ways of assessing the yield point from the load-displacement curve. The first method (called method (a) in the standard) is used when the load-displacement curve has two well-defined linear parts, which is not the case with timber assemblies. The yield point is determined by the intersection of two lines drawn from these two linear parts. The second method (called method (b) in the standard, see Fig. 3) gives a more precise rule on how to draw such lines. The first line is drawn through the points 10% and 40% of the peak load F_{max} on the curve, while the second line is the tangent to the graph that have a slope of 1/6 of the first line slope. The yield load and slip are then determined at the intersection between these two lines.

With regards to the assessment of the ultimate displacement the standard defines three criteria:

a failure;
b the displacement related to the 80% of the peak load (after peak load and for a slip of less than 30mm);
c a joint slip of 30mm.

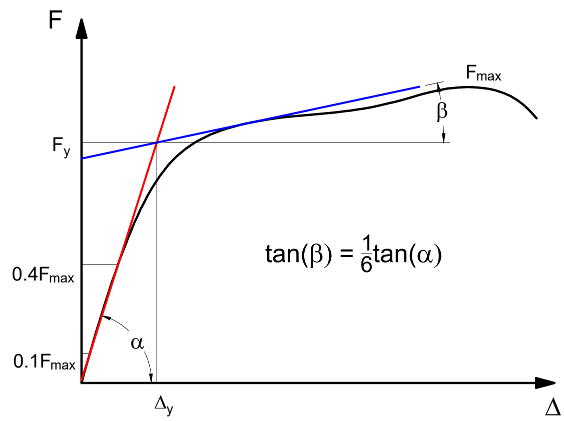

Figure 3. Definition of yield point according to EN 12512 method (b)

2.2.2. Yasumura & Kaway

A commonly adopted method is the so called Yasumura & Kawai procedure Yasumura (1997). According to this method the first line is drawn through the points 10% F_{max} and 40% F_{max} (red line in Fig. 4). The second line is drawn through points corresponding to 40% F_{max} and 90% F_{max}, and is then translated so that the line is tangent to the load-displacement curve (blue line in Fig. 4). The intersection between the two lines gives the yield load. To retrieve the yield slip, the yield load value is projected horizontally onto the load-displacement curve.

The ultimate slip is defined as the one corresponding to 80% of F_{max} on the decreasing part of the load envelope curve. Finally, the ultimate strength F_u is calculated imposing the equivalence of the deformation energies of the load envelope curve and the elasto-plastic curve (orange curve in Fig. 4).

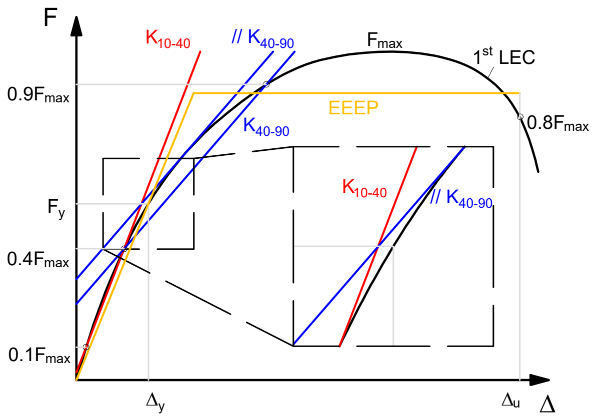

Figure 4. Definition of yield point according to Yasumura & Kawai

2.2.3. EEEP curve approach

The test method in ASTM E2126 has as background Foliente and Zacher (1994), Foliente *et al.* (1998), and contemplate the use of an equivalent energy elastic-plastic curve (EEEP). The method has been included in Casagrande *et al.* (2019) which contain a revision proposal for the EN 12512:2001+A1:2005 standard. The EEEP curve, which is bilinear and represents perfect elastic-plastic behaviour of an assembly, is derived such that the area below the test curve is equivalent to the area under the bilinear curve, see Fig. 5. The first line corresponds to the initial elastic stiffness, and goes through the point 10% and 40% of the peak load F_{max}. The yield load (F_y) is calculated using the following formula, imposing the equivalence of the areas under the two curves:

$$(1) \qquad F_y = \left[\Delta_{failure} - \sqrt{\left(\Delta^2_{failure} - \frac{2w_{failure}}{K}\right)}\right] K$$

Where $\Delta_{failure}$ is the ultimate slip, $w_{failure}$ is energy dissipated before reaching failure (i.e., the area below the curve) and K is the elastic stiffness.

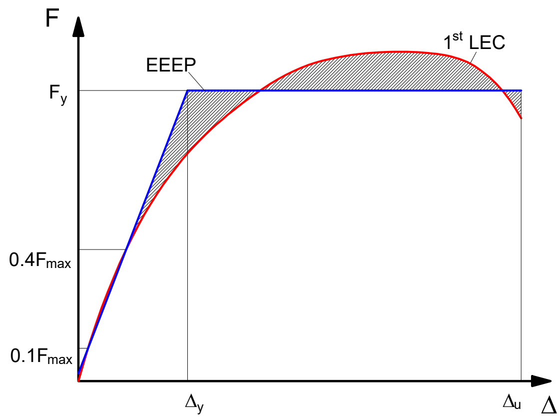

Figure 5. Definition of the EEEP curve (blue) with 1st LEC (red)

While the ASTM E2126 standard considers just one criterion for the definition of the ultimate slip (the slip corresponding to 80% of F_{max}), the revision proposal presented in Casagrande *et al.* (2019) considers three criteria, revising criterion c) of EN 12512:2001+A1:2005:

c The displacement characterized by a strength degradation factor β_{sd} equal to or lower than $\beta_{sd,min}$ whichever occurs first.

The meaning of the non-dimensional coefficient β_{sd} is explained in Fig. 6. This is in accordance with the existing regulations in Eurocode 8 section 8.3 (3)P, which could be interpreted as an implicit definition of the strength degradation factor. The importance of taking into account the strength degradation of the dissipative zones is underlined in Follesa *et al.* (2018), where the value of the strength degradation is set to $\beta_{sd} = 0.8$ and introduced in the calculation of the design strength of a dissipative zone:

$$F_{Rd,d} = k_{mod} \cdot \beta_{sd} \cdot \frac{F_{Rk,d}}{\gamma_m} \quad (2)$$

Where k_{mod} is the modification factor for duration of load and moisture content and γ_m is the safety factor for material properties.

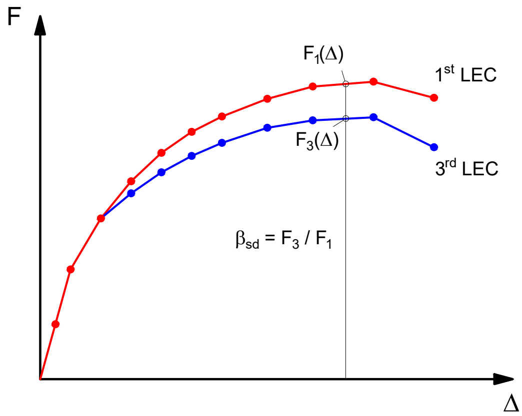

Figure 6. Definition of strength degradation factor

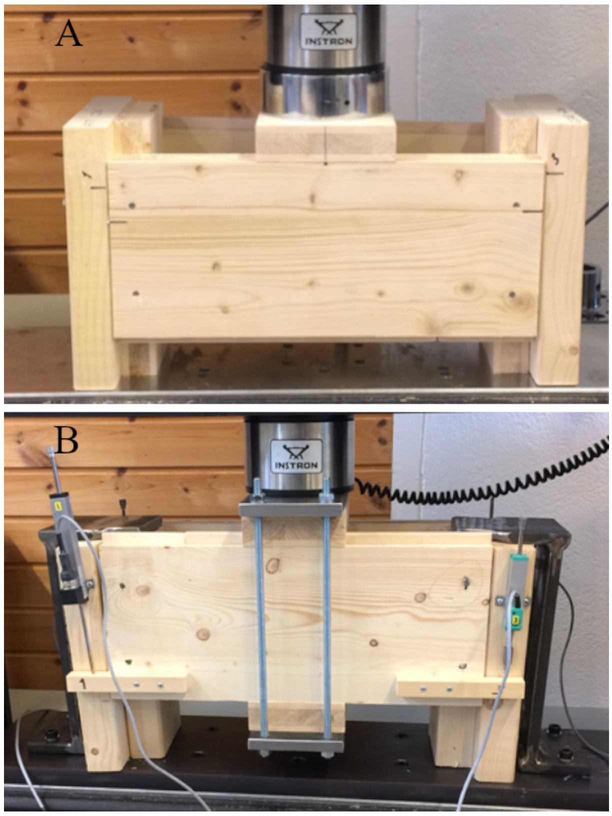

Figure 7. **(A)** Monotonic test set-up; **(B)** Cyclic test set-up

2.3. Experimental investigation

2.3.1. Test set-up and test procedure

Monotonic tests were performed according to the loading procedure presented in EN 26891:1991. Cyclic tests were instead performed according to the procedure presented in EN 12512:2001+A1:2005.

The specimens were positioned centrally under the load cell to avoid any unwanted eccentricity, see Fig. 7A and Fig. 7B). The loads were measured with a load cell placed between the actuator and the specimen. The displacements were instead measured with displacements transducers placed as close as possible to the interface between the panel and the sill, see Fig. 7B.

For the monotonic tests the displacement rate was set as 2 mm/min in the beginning. After the first test, the displacement rate was adjusted to 4 mm/min to adhere to the correct testing time based on EN 26891:1991. Finally, the displacement rate was adjusted once more after F_{est} and set to 5,8 mm/min.

For the cyclic tests a yield slip, $V_{y,est}$, had to be calculated. The value was retrieved from the results of the monotonic tests. The displacement rate for all the tests was 12 mm/min = 0,2 mm/sec, which is the maximum rate, according to EN 12512:2001+A1:2005. Furthermore, a clamping system was produced for the cyclic test set-up. This to maintain the specimen on the base-plate of the machine, during the tension forces pulling it upwards. The steel clamping system and the size of the elements were chosen to minimize the deformations of the steel parts.

Table 1 provides an explanation for the nomenclature of the tested specimens, while Table 2 provides an overview of the configurations for the monotonic and cyclic tests.

3. Results and discussion

3.1. General discussion

The results of the test conducted are discussed in the following section. During the testing none of the specimens showed sudden failures with very significant loss of strength. However,

X (Orientation)	Y (Connector type)	Z (Sill type)	a (Load)
A = 60°to outer panel	N = Nail	S = SWP	s = monotonic
H = 90°to outer panel	S = Screw	T = Solid Timber	c = cyclic

Table 1. Overview of specimen labels

Test Type	Connector	Angle	Sill	n°
Monotonic & Cyclic	Screw	90°	ST	5
			SWP	5
		60°	ST	5
			SWP	5
	Nail	90°	ST	5
			SWP	5
		60°	ST	5
			SWP	5
N_{TOT}				40 (Monotonic)
				40 (Cyclic)

Table 2. Test configurations

after the testing procedures were completed each specimen was disassembled, and in some cases a rupture of the connector was observed. Every fastener had failed either according to failure modes (d), (e) or (f) of the European Yield Model (EN 1995-1-1:2004/A2:2014), meaning with the formation of at least one plastic hinge, see Fig 8A. Most likely, when the connectors had fractured, the friction between the TW element and the sills were holding the specimen together, with quite significant forces.

The load-displacement curves for the monotonic tests are presented in Fig 9. The graph shows the mean load-displacement curve for each configuration so as to obtain a graphical comparison between these. Table 3 reports the mechanical properties, calculated according to EN 26891:1991 for the static tests; Table 4 reports instead the results in terms of mechanical properties for the cyclic tests, which were calculated according to the different methods discussed in section 2.2. On the left hand side of Fig 10, 11 and 12 the hysteresis curves of some specimens are shown along

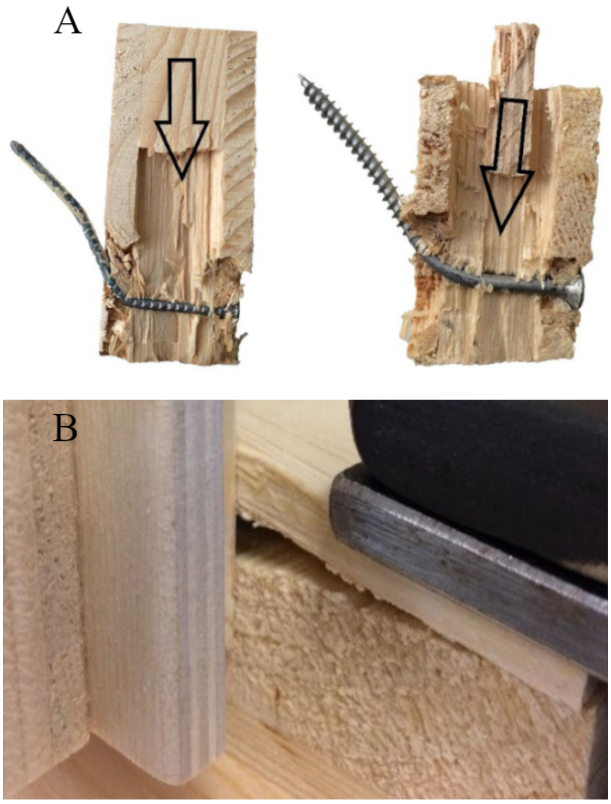

Figure 8. **(A)** Failure modes; **(B)** Detail of the separation between the lamellas of the SWP sill

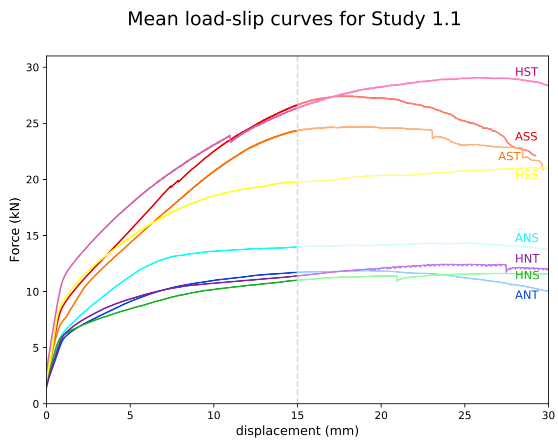

Figure 9. Mean load-slip curves for the static tests

with the corresponding load envelope curves for each cycle. On the right hand side, instead, the load envelope curves with some of the properties evaluated according to the different assessment methodologies are shown.

For both the static and cyclic tests, when the connectors were inserted with a 60°angle, ST sills and SWP sills showed a similar behaviour, with the latter showing slightly better results in terms of strength and stiffness, and the former generally better ductility ratios. However, the results in terms of ductility are very dependent on the method used to assess the mechanical properties, as one can observe in Table 4.

When the connectors were inserted with a 90°angle, strength and stiffness values was observed to be higher for ST sills. This is most likely due to the fact that the connectors frequently penetrated the lamellas close to the glue line in the SWP sill, which resulted in a separation of these when the loads were applied, see Fig 8B. SWP sills however highlighted a more ductile behaviour than ST sills under cyclic loading.

Generally speaking, connectors inserted with a 60°angle showed slightly higher strength and stiffness values, while those inserted horizontally (90°) showed a more ductile behaviour. However, from both Fig 9 and Table 3, it is also clear that the insertion of the connectors with an angle of 60°does not lead to a significant increase in terms of stiffness and shear capacity. This happens because the withdrawal capacity of the connectors is activated only when uplift forces are acting on the connection. For the shear test set-up, in fact, the shear plane at the interface between the element and the sill is not affected by the inclination of the screws or nails. Consequently, the increase in the resistance due to the inclination of the screws is not noticeable.

Furthermore, the use of SWP sills instead of ST sills did not increase the capacity and stiffness substantially, especially when connectors of bigger diameter were used. In fact, quite often the insertion of the screws with a 90°angle, made the mechanical properties poorer. As already pointed out, this is related to several cases of lamella separation, where the bigger point of the screws connectors hit the lamellas at the glue line forcing a separation during the loading procedures. This behaviour was even more prominent when the specimens were tested for uplift forces.

Finally, screw connectors were stronger and stiffer than nail connectors, while the latter were more ductile, as it was expected. It is worth to point out that often one specimen per configuration showed a behaviour that differed from the other, which contributed to the rather high values of the standard deviations of the properties reported in the tables.

3.2. Comparison of the yield point assessment and ductility ratios

It is of interest to compare the results of the cyclic tests in terms of yield slip, yield load and ductility ratios, and discuss the advantages and disadvantages of the methods used to assess these properties. Since the ductility is defined as the ratio between the ultimate slip and the yield slip, its values are strongly influenced by the method used to evaluate both these quantities.

Regarding the yield point, the results from the EEEP method are located always off the curve in regions where plastic deformations have already occurred, and gives therefore the highest values in terms of yield load and displacement (see Fig 10, Fig 11, Fig 12. The results from the 1/6 procedure and the Yasumura & Kaway procedure are closer to each other, except for specimens with a relatively lower initial stiffness. When the initial stiffness is lower in fact, the yield point derived from the 1/6 procedure tends to go off the load-displacement graph, and closer to the yield point determined from the EEEP procedure (see Fig 11). As for the Y&K procedure, the initial stiffness does not affect the yield point location, which always stays on the curve. From a computational point of view however the EEEP method is the easiest method to program, since it does not involve the process of finding a line tangent to the load envelope curve.

A novelty of Casagrande *et al.* (2019) is the revision of criterion c) of the EN 12512:2001+A1:2005. This criterion was introduced in order to take into account the degradation of the resistance capacity typical of assemblies subjected to cyclic loading. This condition should grant results that are more conservative in terms of ultimate slip and ultimate load, and is consistent with the new provisions for Capacity Design rules proposed in Follesa *et al.* (2018). Both the work in fact underline that the low cyclic fatigue strength represents a key-parameter for the seismic behaviour of timber connections, in order to ensure high ductility and large amount of energy dissipation without a significant loss of strength.

Property	Test group study 1.1							
	ANSs	ANTs	ASSs	ASTs	HNSs	HNTs	HSSs	HSTs
F_y [kN]	6.63 (0.30)	6.05 (0.46)	11.16 (0.85)	10.38 (1.02)	5.92 (0.46)	6.46 (0.32)	9.83 (1.05)	13.03 (0.47)
v_y [mm]	1.18 (0.23)	1.17 (0.27)	2.24 (0.29)	2.08 (0.94)	0.88 (0.21)	1.24 (0.23)	1.29 (0.30)	1.82 (0.44)
F_u [kN]	14.06 (0.59)	11.72 (0.60)	26.65 (1.63)	24.39 (1.55)	11.01 (0.70)	11.40 (0.80)	19.79 (1.21)	26.32 (1.91)
K_{ser} [kN/mm]	5.76 (1.03)	5.32 (0.83)	5.00 (0.27)	5.52 (1.44)	6.93 (1.21)	5.31 (0.83)	7.77 (1.00)	7.45 (1.58)

Table 3. Results from monotonic tests - Mean values and standard deviations in brackets

Method	Property	Test group study 1.2							
		ANSc	ANTc	ASSc	ASTc	HNSc	HNTc	HSSc	HSTc
Y & K	F_y [kN]	3.93 (1.47)	3.90 (0.88)	9.92 (2.46)	7.73 (1.03)	3.40 (0.39)	4.35 (0.90)	6.31 (0.97)	7.26 (1.59)
	v_y [mm]	2.00 (0.69)	2.44 (0.79)	4.83 (1.65)	2.58 (0.71)	1.60 (0.67)	2.64 (0.80)	2.50 (0.82)	2.76 (0.30)
	F_u [kN]	7.45 (0.97)	7.06 (0.46)	17.89 (1.15)	15.47 (1.03)	6.49 (0.44)	7.47 (0.63)	13.37 (0.91)	14.97 (1.27)
	D [-]	8.38 (4.72)	6.04 (1.54)	4.70 (1.87)	7.14 (1.74)	10.50 (3.26)	5.68 (1.72)	9.13 (1.76)	6.76 (0.86)
1/6 Procedure	F_y [kN]	5.32 (0.47)	3.62 (2.01)	12.74 (2.61)	11.29 (2.07)	3.42 (0.34)	4.90 (0.96)	9.31 (2.57)	11.30 (0.95)
	v_y [mm]	2.65 (0.59)	1.82 (1.17)	5.80 (1.43)	3.78 (1.03)	1.73 (0.51)	2.72 (0.93)	4.05 (0.91)	5.40 (0.35)
	F_u [kN]	7.34 (0.64)	6.74 (0.39)	16.05 (1.05)	14.17 (1.24)	6.52 (0.50)	6.89 (0.63)	12.23 (0.42)	13.92 (1.03)
	D [-]	5.50 (1.04)	9.68 (4.56)	3.70 (0.76)	4.88 (1.38)	9.55 (2.87)	5.60 (1.94)	5.65 (1.62)	3.48 (0.15)
EEEP	F_y [kN]	6.87 (0.77)	6.34 (0.73)	17.50 (1.19)	15.15 (0.97)	6.39 (0.42)	6.96 (0.63)	13.30 (0.75)	14.63 (0.89)
	v_y [mm]	3.50 (0.61)	3.62 (1.92)	7.70 (0.80)	5.20 (0.61)	3.63 (1.49)	4.00 (1.06)	5.53 (0.42)	7.05 (0.58)
	F_u [kN]	6.87 (0.77)	6.34 (0.73)	17.50 (1.19)	15.15 (0.97)	6.39 (0.42)	6.96 (0.63)	13.30 (0.75)	14.63 (0.89)
	D [-]	3.28 (0.61)	3.62 (1.72)	2.40 (0.29)	2.98 (0.44)	4.63 (2.23)	2.86 (0.96)	3.58 (0.56)	2.28 (0.15)

Table 4. Results from cyclic tests - Mean values and standard deviations in brackets

For the specimens tested under cyclic loading the application of the revised condition c) indeed influenced the results. Very often in fact condition c) was the decisive one to determine the ultimate slip. On the contrary, when the 1/6 procedure was applied condition b) was the decisive one. This can be observed comparing the ductility ratios in Table 4. The ductility ratios obtained from the revision proposal are in fact always lower compared to those calculated according to the current version of the standard.

An observation worth noticing is that, referring to the definition given in EN 1998-1:2004/A1:2013 (clause 8.3(3)P), the differences in the ductility ratios between the different approach leads to a different classification of the joints for several of the tested groups. This is due not only to the fact that the calculated ultimate slip is very often lower with the adoption of the new method, but also due to the yield slip being always grater. As already pointed out, using the EEEP method, the yield point will be located far of the curve and in a region where plastic deformations have already occurred, overestimating the yield slip and yield load. The consequence of this is that, inevitably, the ductility ratios will be lower.

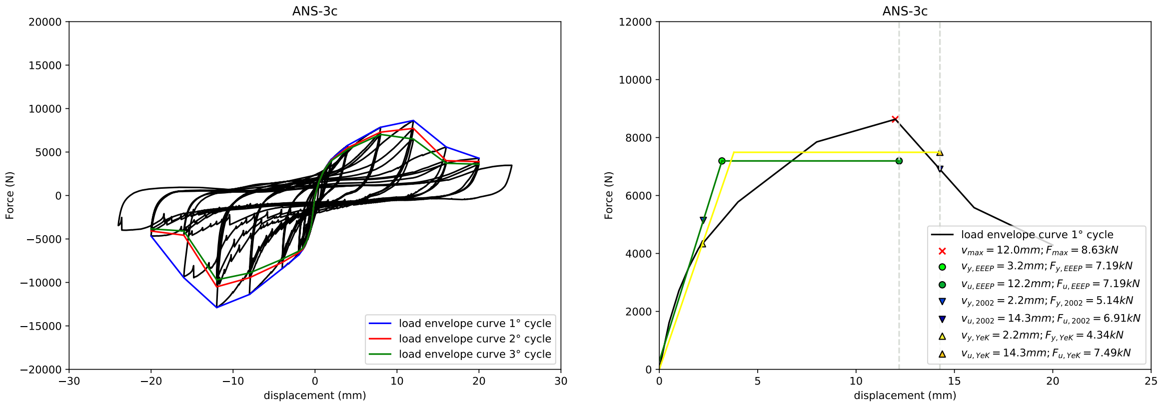

Figure 10. Load envelope curves and hysteresis curves for specimen ANS-3

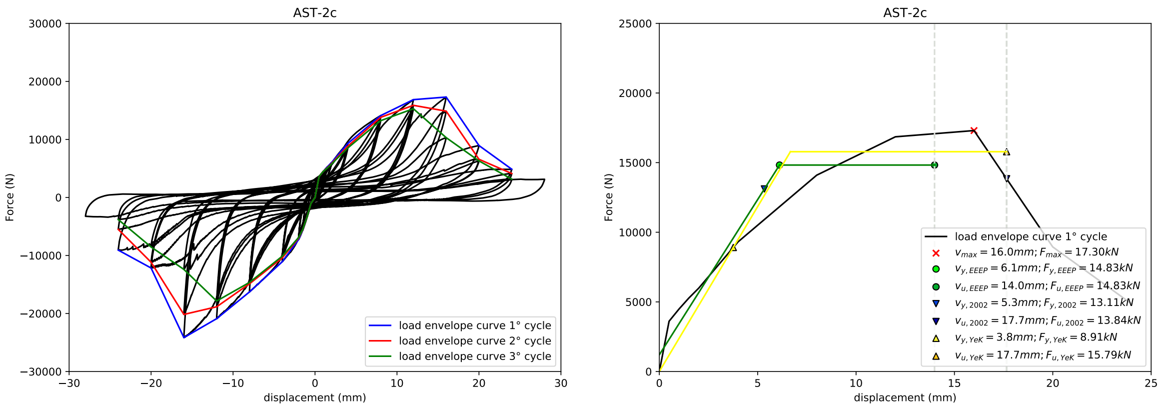

Figure 11. Load envelope curves and hysteresis curves for specimen AST-2

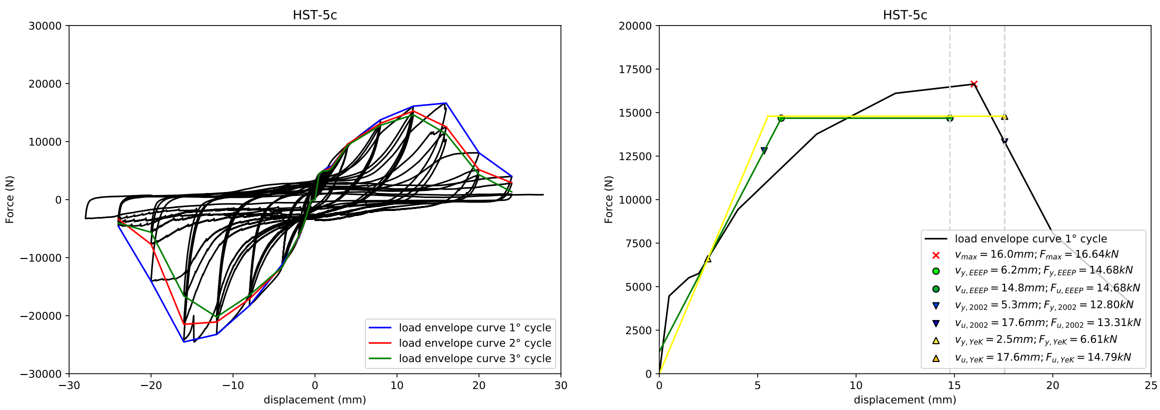

Figure 12. Load envelope curves and hysteresis curves for specimen HST-5

4. Conclusions

In the continuous efforts to maintain the Eurocodes at the forefront of engineering knowledge and developments of the construction market, CEN/TC 250 is currently preparing the revision of the existing set of codes. Assessing the link between product standards or other European standards, in particular with regard to any discrepancies, is one of the main goals in order to create the conditions for a harmonised system of general rules. In this context drafts for the revision of both EN 1998-1:2004/A1:2013 and EN 12512:2001+A1:2005 are under discussion by the responsible subcommittee.

As already mentioned, in order to perform a design in accordance to EN 1998-1:2004/A1:2013, information about mechanical properties of dissipative zones are needed. For timber connections these may be determined from experimental tests in accordance with EN 12512:2001+A1:2005. The link between EN 1998-1:2004/A1:2013 and EN 12512:2001+A1:2005 is even tighter in the draft under discussion as suggested by Follesa *et al.* (2018). The proposal for the revision of the current version of the test methods standard presented in Casagrande *et al.* (2019) introduces, in addition to a slightly revised procedure to perform the tests, new methods to derive the needed mechanical properties. The main novelty are the introduction of a revised condition to determine the ultimate slip (and ultimate load), and a different approach to calculate the yield point. The latter is in fact derived through the definition of the EEEP curve as in ASTM E2126. The yielding load, F_y, and the yielding displacement, v_y, are obtained so that the areas under the load-displacement curve between the origin and the ultimate displacement is the same for the envelope curve and the EEEP curve.

It is the opinion of the authors that the introduction of this procedure makes the assessment of the mechanical properties more robust from a computational point of view, since the calculations are easier to program; furthermore, a given data set will always yield the same results. A weakness of the methods provided by the current version of the standard is in fact that, being based on a more graphical approach (i.e. move a line until it is tangent to the curve), they are more difficult to program and could yield different results if a data set is given to different operators. Moreover, it is important to take into account strength degradation in order to ensure high ductility and a large amount of energy dissipation without a significant loss of strength. An argument against the EEEP method however is that the yield point will be located far off the curve and in a region where plastic deformations have already occurred, overestimating the yield slip and yield load. Additionally a consequence is that the ductility values will always be lower compared to those calculated with the current prescription (or those outlined in Yasumura (1997), and this could perhaps be seen as too punitive.

5. Acknowledgements

The authors would like to thank Termowood AS for providing the testing material and financially support the research.

REFERENCES

ASTM E2126 (2011) *Standard test methods for cyclic (reversed) load test for shear resistance of vertical elements of the lateral force resisting systems for buildings*. *Technical report*, ASTM.

EN 12512:2001+A1:2005 (2001) *Timber Structures - Test Methods - Cyclic Testing of Joints Made with Mechanical Fasteners*. *Standard*, CEN.

EN 13353:2008+A1:2011 (2011) *Solid wood panels (SWP) - Requirements*. *Standard*, CEN.

EN 1995-1-1:2004/A2:2014 (2014) *Eurocode 5: Design of timber structures - Part 1-1: General - Common rules and rules for buildings*. *Standard*, CEN.

EN 1998-1:2004/A1:2013 (2013) *Eurocode 8: Design of structures for earthquake resistance - Part 1: General rules, seismic actions and rules for buildings*. *Standard*, CEN.

EN 26891:1991 (1991) *Timber structures - Joints made with mechanical fasteners - General principles for the determination of strength and deformation characteristics (ISO 6891:1983)*. *Standard*, CEN.

EN 338:2016 (2016) *Structural timber - Strength classes*. *Standard*, CEN.

Foliente G, Karacabeyli E and Yasumura M (1998) International test standards for joints in timber structures under earthquake and wind loads. In *Proc., Structural Engineers World Congress*.

Foliente G and Zacher E (1994) Performance tests of timber structural systems under seismic loads. In *Analysis, Design and Testing of Timber Structures Under Seismic Loads, Proc., Research Needs Workshop. GC Foliente, ed., University of California Forest Products Laboratory, Richmond, California*, pp. 3–23.

Follesa M, Fragiacomo M, Casagrande D, Tomasi R, Piazza M, Vassallo D, Canetti D and Rossi S (2018) The new provisions for the seismic design of timber buildings in europe. *Engineering Structures* **168**: 736–747.

ISO 554:1976 (1976) *Standard atmospheres for conditioning and/or testing – Specifications*. *Standard*, International Organization for Standardization.

Muñoz W, Mohammad M, Salenikovich A and Quenneville P (2008) Yield point and ductility of timber assemblies: A need for a harmonised approach. In *Proc. Annu. Conf. Can. Soc. Civ. Eng*, vol. 2, pp. 1146–1155.

Pasca D, Myrvhold CA, Hø ibø OA, Nyrud A and Tomasi R (2019) Assessment of the connection properties of a prefabricated wooden sandwich panel under static and cyclic loads. In *Report of the IABSE Symposium Guimares 2019 - Towards a Resilient Built Environment Risk and Asset Management*.

Piazza M, Polastri A and Tomasi R (2011) Ductility of timber joints under static and cyclic loads. *Proceedings of the Institution of Civil Engineers-Structures and Buildings* **164(2)**: 79–90.

Piazza M, Tomasi R, Grossi P, Costa AC and Candeias PX (2015) Seismic performance of timber buildings: the series project. *Proceedings of the Institution of Civil Engineers-Structures and Buildings* **168(11)**: 788–802.

Casagrande D, Bezzi S, D′Arenzo G, et al. (2019) A methodology to determine the seismic low-cycle fatigue strength of timber connections. *Construction and Building Materials (accepted).*

Termowood AT (2007) European patent number ep1963593. *International publication number WO* **69908**: A1.

Yasumura M (1997) Evaluation of wood framed shear walls subjected to lateral load. *Proceedings of the 30th CIB-W18, Vancouver, Canada, 1997* .